2024 32nd Southern African Universities Power Engineering Conference (SAUPEC) | 979-8-3503-7134-5/24/$31.00 ©2024 IEEE | DOI: 10.1109/SAUPEC60914.2024.10445060

Performance Evaluation Of Grid-scale Battery Energy Storage System Employing Virtual Synchronous Generator Control For Grid Code Compliance In Weak Grids

Karabo Senyane
School of Electrical and Information Engineering
University of the Witwatersrand
Johannesburg, South Africa
karabo.senyane51@gmail.com

John Van Coller
School of Electrical and Information Engineering
University of the Witwatersrand
Johannesburg, South Africa
john.vancoller@wits.ac.za

Lesedi Masisi
School of Electrical and Information Engineering
University of the Witwatersrand
Johannesburg, South Africa
lesedi.masisi@wits.ac.za

***Abstract*—This document is on the design and testing of a grid-scale Battery Energy Storage System (BESS) employing Virtual Synchronous Generator (VSG) control grid-forming scheme. The BESS is rated 60 MWh/50 MW. The simulations were conducted using MATLAB/Simulink/Simscape software. The protection functions and the associated protection relays needed to achieve these functionalities are presented. The approach adopted can apply to any relevant standard or grid code associated with a Transmission System Operator (TSO) internationally, however, the local grid codes in the context of South Africa were used. The system is designed to be compliant with the document Grid Connection Code for Battery Energy Storage Facilities (BESF) connected to the Electricity Transmission System (TS) or the Distribution System (DS) in South Africa and is classified under Category C as defined in the same document. The system was able to adjust both its active and reactive power outputs accordingly in response to load reduction conditions in the network. Furthermore, for local fault conditions, it was able to ride-through transient faults and trip and disconnect for permanent faults. For these two cases the BESS protection functionality serves as primary protection. The system was also able to trip and disconnect for remote permanent faults where the associated protection functionality is utilised as back-up protection.**

***Index Terms*—grid stability, BESS, grid-forming inverters, grid code, weak grid**

I. Introduction

Power grids worldwide are undergoing a major transition from the synchronous generator dominated technology associated with fossil-fuel generators to generation and storage technology based on Inverter Based Resources (IBRs). BESS is meant to play an integral role in mitigating the intermittency associated with large-scale solar and wind power generation plants. There are numerous grid-forming techniques in the literature, however, the focus of this work shall be on Virtual Synchronous Generator (VSG) technology. Models in both Root Mean Squared (RMS) (phasor) and Electro-Magnetic Transient (EMT)-based simulation software packages are increasingly becoming important tools in the field of power systems. These models are important for grid-integration studies in order to assess the stability of newly-built or modified components of the grid such as generators and BESS.

II. Literature review

In [1], Vilmann *et al* investigated the stability of wind farms when they are integrated into parts of the grid considered weak. The frequency and voltage compliance capabilities of three grid-forming techniques namely: droop control, Virtual Synchronous Machine (VSM) and synchronverter were investigated and benchmarked. The procedure followed was that of quantifying the performance during a contingency of a frequency disturbance, with sensitivity to the Short Circuit Ratio (SCR), X/R ratio and the inertia constant H. The conclusion of the investigation was that the VSM is the most compliant grid-forming control technique. In [2], Sang *et al* reviewed the history of some of the common grid-forming control technologies which are the VSG and the synchronverter. Detailed descriptions of the two is outlined in [3] and [4] respectively. In [5], Alsokhiry *et al* investigated the limitations of Voltage Source Converters (VSC) in weak AC grids from a voltage stability point of view. The conclusion from the analysis was that the maximum active power that the VSC can exchange with a weak AC grid is determined by voltage stability limits. The simulations were conducted using MATLAB/Simulink. In [6], a comprehensive review of grid-forming pilot projects and demonstrations that have been implemented worldwide was undertaken. The projects include BESS, HVDC systems, wind farms and hybrid plants. A comparison study was also undertaken where the similarities and differences between the projects were highlighted. A similar review of grid-scale BESS grid-forming projects, already in deployment or under construction worldwide, was conducted and listed in [7]. In [8] Minnaar *et al* investigated issues of power quality as pertains to grid code compliance in South Africa, with a focus on harmonic emissions. However, there was not much

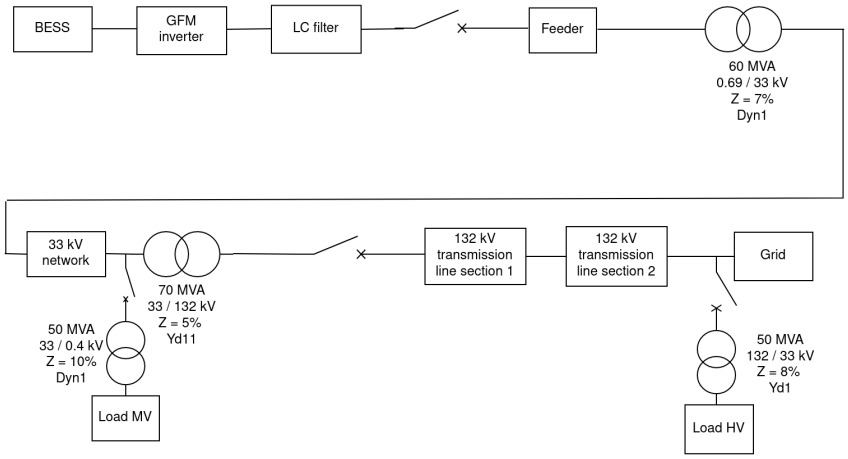

Fig. 1. Single line diagram for investigated network

focus on BESS technology in particular and no conduction of simulations to test for grid code compliance. The authors in [9] also looked into technicalities of grid codes and compared the South African grid code for Renewable Power Plants (RPPs) to those of other Transmission System Operators (TSOs) that operate within other countries with a main focus on European countries. The TSOs include Energinet in Denmark, EirGrid in Ireland and SONI in Northern Ireland, National Grid in the United Kingdom and TenneT in Germany. However, there were no simulations undertaken in order to evaluate the dynamic performance of the RPPs or BESS against grid code compliance for any of the TSOs.

There has been limited studies in performance evaluation of grid-forming BESS for grid code compliance in weak grids both internationally and locally, in the context of the grid in South Africa. This paper seeks to fill in this gap.

III. Methodology

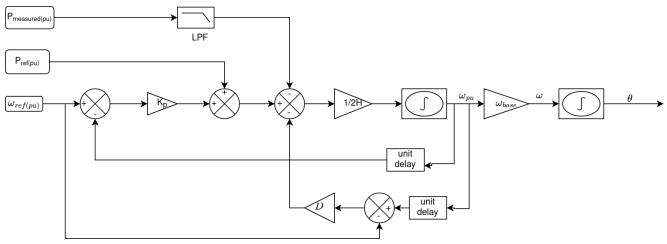

Fig. 2. Control block for implementation of P-f droop, inertia and damping for the BESS inverter

Fig. 1 shows the single line diagram of the network used in the investigation. The SCR at the grid interface point is 3, which corresponds to a weak grid condition. The core control module for the VSG is shown in Fig. 2. It includes damping, with the corresponding damping constant denoted by the letter D, active power vs frequency droop constant denoted by the letter K_p and inertia constant denoted by the letter H. Other control blocks such as those that implement reactive power vs voltage droop are not shown. All the inverter control techniques are implemented in the direct-quadrature-zero (dq0) domain. The Park Transformation is utilised to transform the network variables from the conventional three-phase *abc* reference frame to the *dq0* rotating reference frame, and the inverse Park Transformation is utilised to re-transform them after control and manipulation.

For the overall control loops the cascaded voltage and current control technique was implemented and extensive explanation of the comprehensive VSG control loops is documented in [2]. In cases where the local grid code does not exist or is underdeveloped, international standards such as the IEEE Standard for Interconnection and Interoperability of Inverter-Based Resources (IBRs) Interconnecting with Associated Transmission Electric Power Systems (IEEE 2800-2022), or other well-developed grid codes such as that for National Grid in the United Kingdom, can be used as a guideline for testing for compliance. However, for the focus of this particular investigation the South African grid code document for BESS compliance is well-developed enough to be used as a guideline. The base values for the per unit system are derived from a 50 MVA base and a base voltage of 0.69 kV.

TABLE I
BESS Voltage-time pair values for ride-through conditions

Voltage (p.u)	time (s)	Voltage (p.u)	time (s)
$0 \leq V < 0.10$	0.15	$0.60 \leq V < 0.70$	1.46
$0.10 \leq V < 0.20$	0.37	$0.70 \leq V < 0.80$	1.67
$0.20 \leq V < 0.30$	0.59	$0.80 \leq V < 0.85$	2.00
$0.30 \leq V < 0.40$	0.80	$0.85 \leq V < 0.90$	20.0
$0.40 \leq V < 0.50$	1.02	$0.90 \leq V \leq 1.08$	normal operation
$0.50 \leq V < 0.60$	1.24	$1.08 < V \leq 1.20$	2.00

Both Table I and Table II are extracted from graphs in [10]. These tables show the ranges for both the voltage and frequency and the corresponding minimum trip times which are set in the protection and control modules of the BESS.

TABLE II
BESS FREQUENCY-TIME PAIR VALUES FOR RIDE-THROUGH CONDITIONS

Frequency (Hz)	Trip time (s)	Frequency (Hz)	Trip time (s)
$47 < f$	0.20	$49 \leq f \leq 51$	normal operation
$47 \leq f < 47.5$	6.0	$51 < f < 51.5$	60
$47.5 \leq f < 48$	10	$51.5 \leq f$	4.0
$48 \leq f < 49$	60		

IV. RESULTS AND DISCUSSION

A. Load reduction test

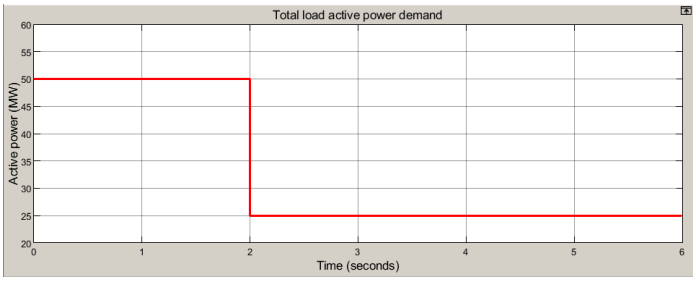

Fig. 3. Total system load excluding network losses

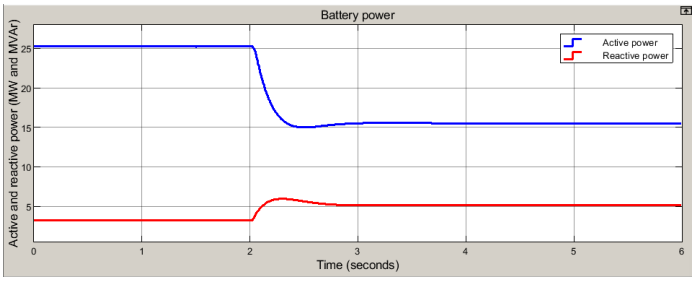

Fig. 4. Battery power - load reduction test

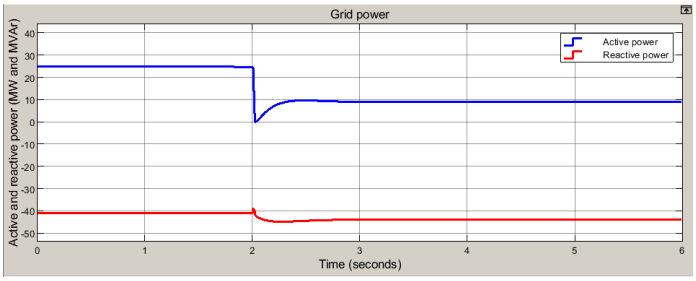

Fig. 5. Grid power - load reduction test

Fig. 3 shows a triggering event in the network whereby the load on the HV side connected through a 132/33 kV transformer is disconnected at time 2 seconds. From the BESS point of interconnection, this is equivalent and has the same effect as the switching on of a generator that supplies the equivalent amount of active power to that of the disconnected load being brought online and partaking in the supply of active power in the network. Both these events would require a reduction of active power supplied by the BESS and other generators in order to ensure that the demand and supply of active power is closely matched. Fig. 4 and Fig. 5 show a reduction in active power supply by both the battery and the grid supply respectively in response to this event. This is to prevent an oversupply of active power in the network which can result in an over-frequency event. The BESS active power reduction is achieved through reduction of the current injected by the inverter as shown in Fig. 8. The voltage slightly drops from 1.035 p.u before the event to 0.992 p.u as shown in Fig. 6 so the reactive power supplied slightly increases in order to boost the voltage to a value closer to 1.00 p.u. Both the values of voltage and frequency before and after the event remained within the permissible range of normal operation as required by the grid code and shown in Table I and Table II respectively.

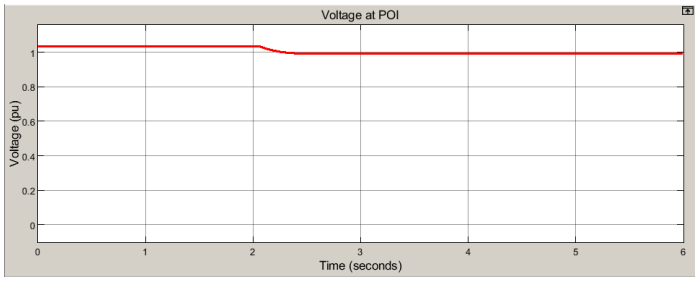

Fig. 6. Voltage at the POI - load reduction test

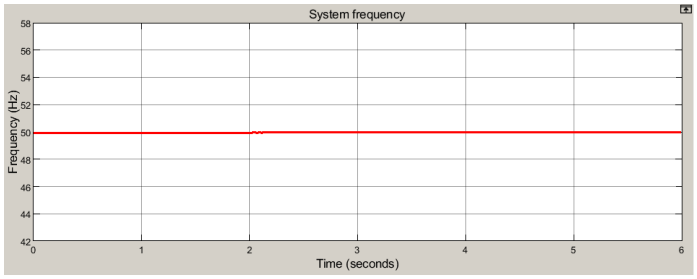

Fig. 7. System frequency - load reduction test

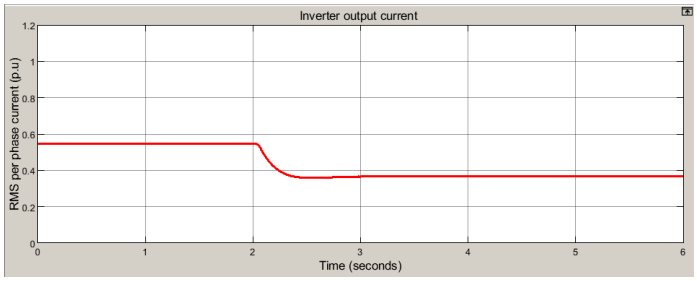

Fig. 8. Inverter current output - load reduction test

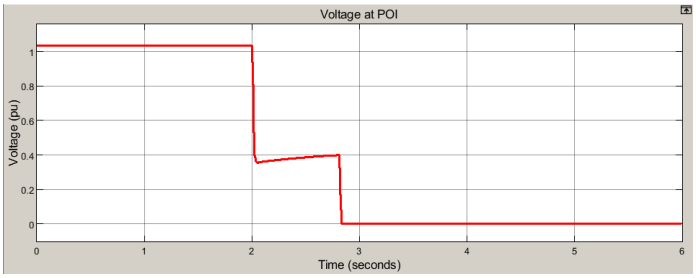

Fig. 9. Voltage profile - permanent remote fault

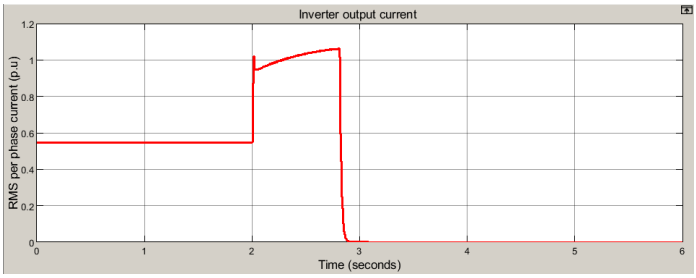

Fig. 10. Inverter current - permanent remote fault

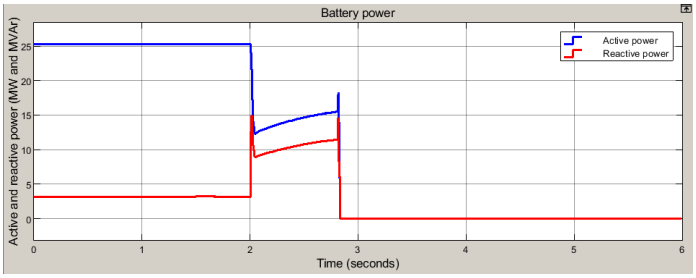

Fig. 11. Battery output power - permanent remote fault

B. Permanent remote fault

Fig. 9 – 11 show the response of the BESS when a three-phase-to-ground fault is applied at time 2 seconds on the 132 kV line. The fault conditions and effects propagate from the 132 kV line section to the BESS through other network components. These components, which include the transformers and the 132 kV line as shown in Fig. 1, have associated protection functions which, under normal conditions, act first to clear the fault before it reaches the BESS. The assumption is that for this particular test case this primary protection is disabled so that the capability of the BESS protection modules is evaluated in responding appropriately as back-up protection for remote faults.

The fault causes a voltage dip as shown in Fig. 9 where the voltage drops to 0.35 p.u, this in turn initiates a trip signal 0.8 seconds after the fault onset. This results in the disconnection and shut-down of the BESS. This is the expected trip time associated with this particular voltage level as can be confirmed in Table I. In practice, the frequency and voltage ride-through functionality implemented for the BESS can be achieved through one or more Intelligent Electronic Devices (IEDs) as summarised in Table III. All the functionalities in

TABLE III
RELAY FUNCTIONALITY ASSOCIATED WITH BESS

Functionality	Protection relay	ANSI code
Trip due to voltage dips	Under-voltage	27
Trip due to voltage swells	Over-voltage	59
Trip due to under-frequency	Under-frequency	81U
Trip due to over-frequency	Over-frequency	81O

Table III require time coordination in order to incorporate appropriate trip delays associated with a particular voltage level and frequency as depicted in Table I and Table II respectively. The system has built-in current limiting functionality that is designed to activate when the inverter current reaches a value of 1.2 p.u in order to protect the electronic circuitry associated with the converter. The technique implemented for this functionality is the current-saturation method. The fault current only reaches to a peak value of 1.08 p.u before trip as shown in Fig. 10. Fig. 11 shows that for the period of the fault duration, active power decreased while the reactive power increased. This is expected behaviour as standards and grid codes impose consumption or injection of reactive power on BESS inverters in order to support the bus voltage at the connection point [11][12].

C. Permanent fault - local fault

This test is similar to the one performed for a permanent three-phase-to-ground fault. The difference is the location of the fault with respect to the connection point of the BESS. The fault location is the low voltage side (0.69 kV) after the LC filter as shown in Fig. 1.

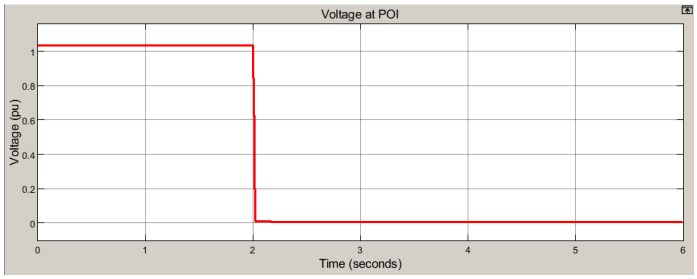

Fig. 12. Voltage profile - permanent local fault

Fig. 12 shows a voltage dip where the voltage drops to 0.01 p.u as a result of the fault condition. The fault current spikes to a value of 1.16 p.u but settles to a steady value of 0.9 p.u for the duration of the fault before a trip signal is issued. Both the active and reactive power supplied by the inverter drop to values close to zero as shown in Fig. 14. This can be attributed to the fact that the voltage value is low and regardless of the current and the phase angle, which all contribute to the active and reactive power, drives both to a value very close to zero. The trip signal was activated 150 milliseconds after the start

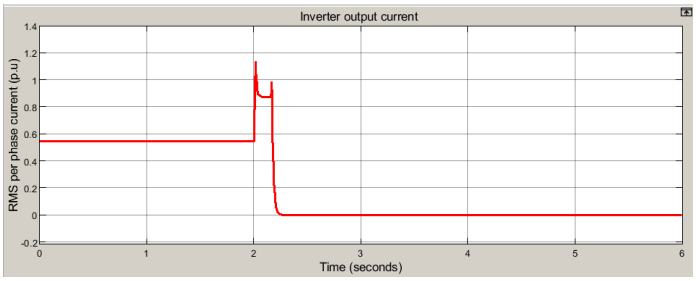

Fig. 13. inverter current - permanent local fault

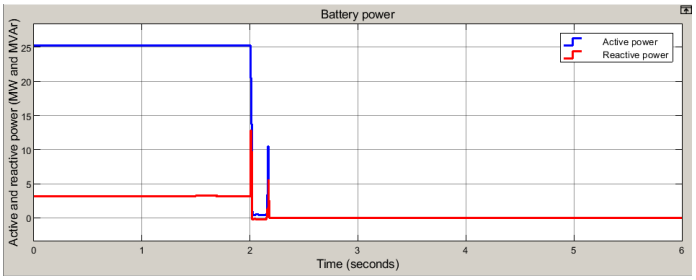

Fig. 14. Battery power profile - permanent local fault

of the fault as per Table I, and confirmed by the behaviour shown in Fig. 12 – 14.

D. Temporary local fault

This test is similar to the permanent local fault test, the difference being the fault duration. The fault is applied for 100 milliseconds, which is less than the 150 milliseconds minimum trip time for this particular voltage level as shown in Fig. 15. The voltage swell in the fault recovery period shortly after the voltage is restored to 1 p.u is a frequently occurring phenomena for IBRs as documented and investigated in [13]. The voltage swell has a peak value of 1.14 p.u, which if sustained for a minimum time of 2 seconds would trigger a trip signal due to over-voltage conditions as required by Table I. However, since it only lasts for a short period before the voltage decays to the pre-fault value there is no trip signal activated.

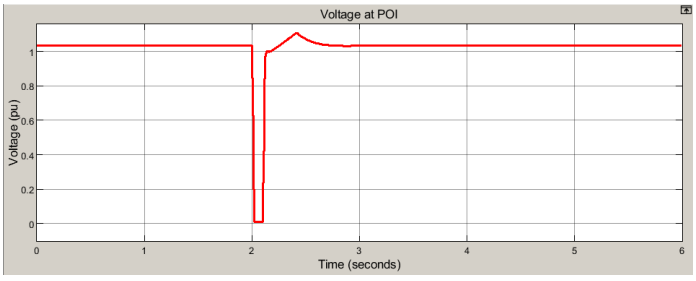

Fig. 15. Voltage profile - temporary local fault

The current spikes to a value of 1.16 p.u and recovers within one second to the pre-fault value as shown in Fig. 16. Both

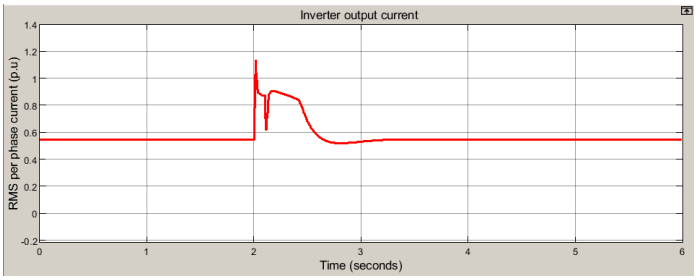

Fig. 16. inverter current - temporary local fault

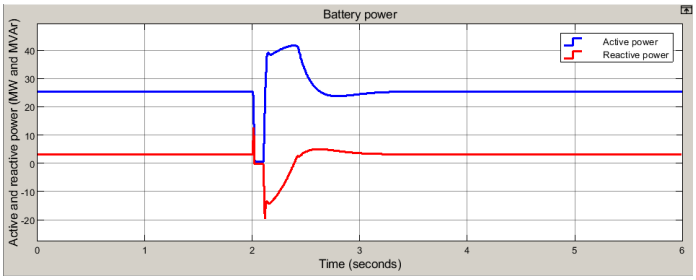

Fig. 17. Battery power profile - temporary local fault

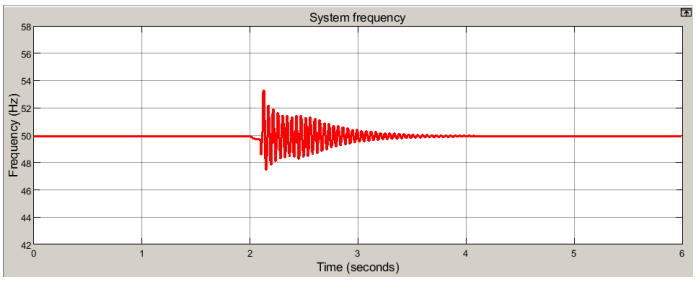

Fig. 18. Frequency signal - temporary local fault

the active and reactive power dip to a value of zero during the fault duration as shown in Fig. 17. In the recovery period, the active power overshoots by more than 60% of the pre-fault value but settles to the correct value within one second. The frequency exhibits some under-damped oscillations that start when the fault is cleared but reasonably decay out within a period of 1.5 seconds to the pre-fault steady-state value as shown in Fig. 18.

A particular aspect to be noted is that the compliance requirements such as Low Voltage Ride Through (LVRT) and frequency ride-through differ in different jurisdictions guided by the relevant grid code. These requirements are dynamic in that they may be tuned and adjusted in the future by system operators and their associated grid code advisory committees in order to ensure overall grid stability as more experience is gained in operating grids dominated by IBRs. For example, the ride-through condition shown in Fig.15 is a requirement for BESS required to comply with ESKOM BESS grid code but the system would be required to trip for the same voltage

dip condition if it was to meet compliance with the Energinet (Denmark) and EirGrid (Ireland) grid codes as compared in [9]. This is because the lowest permissible voltage level during a dip is 0.2 p.u for the former and 0.15 p.u for the latter.

V. Further work and recommendations

- The 132 kV bus which is the grid interface point has a low power factor as shown by the large value for the inductive reactive power in Fig.5. For this, reactive power devices such as Static Var Compensators (SVCs), STATCOMs and other compensating devices can be incorporated for reactive power injection/absorption in order to improve the power factor.
- The BESS interacts with the grid-equivalent network representing the dynamics of the rest of the bulk power grid. It can also be co-located with renewable energy power plants such as large-scale solar and wind farms, especially Type 4 wind turbines which have become a topic of research interest and are constantly being optimised and improved. This is to ensure a more stable hybrid plant consisting of an intermittent energy source and some storage technology for a more reliable and dispatchable overall power output.
- The time-domain graph that depicts the frequency of the system shown in Fig. 18 shows oscillations which are characteristic of an under-damped higher order system with slow decaying oscillations, the variables in the network that affect both the natural frequency and damping ratio of the system can be further investigated to shorten the settling time and to overdamp the frequency oscillations when there is a temporary local fault in the network.
- For simulations, an RMS simulation tool was used, to investigate further some of the phenomena associated with integration of BESS with grid-forming capabilities in power grids an EMT-based simulation tool is recommended.

VI. Conclusion

This paper has presented the performance evaluation of grid-scale BESS that utilises VSG control for grid code compliance in weak grids. The BESS system was able to adjust both reactive and active power output accordingly when there was a requirement in the network for such. It was also able to trip and disconnect for permanent faults initiated in different locations of the network and ride-through transient fault conditions. Further recommendations include conducting the investigation utilising an EMT-based simulation tool.

References

[1] B. Vilmann, P. J. Randewijk, H. Jóhannsson, J. Hjerrild, and A. Khalil, "Frequency and voltage compliance capabilities of grid-forming wind turbines in offshore wind farms in weak ac grids," *Electronics*, vol. 12, no. 5, 2023. [Online]. Available: https://www.mdpi.com/2079-9292/12/5/1114

[2] W. Sang, W. Guo, S. Dai, C. Tian, S. Yu, and Y. Teng, "Virtual synchronous generator, a comprehensive overview," *Energies*, vol. 15, no. 17, 2022. [Online]. Available: https://www.mdpi.com/1996-1073/15/17/6148

[3] H. P. Beck and R. Hesse, "Virtual synchronous machine," in *9th International Conference on Electrical Power Quality and Utilisation*, 2007, pp. 1–6.

[4] Q.-C. Zhong and G. Weiss, "Synchronverters: Inverters that mimic synchronous generators," *IEEE Transactions on Industrial Electronics*, vol. 58, no. 4, pp. 1259–1267, 2011.

[5] F. Alsokhiry, G. Adam, and Y. Al-Turki, "Limitations of voltage source converter in weak AC networks from voltage stability point of view," *International Journal of Electrical Power and Energy Systems*, vol. 119, p. 105899, 2020. [Online]. Available: https://www.sciencedirect.com/science/article/pii/S0142061519332466

[6] R. Musca, A. Vasile, and G. Zizzo, *Grid-forming converters. A critical review of pilot projects and demonstrators*. Elsevier, 2022, vol. 165, p. 112551. [Online]. Available: https://www.sciencedirect.com/science/article/pii/S1364032122004506

[7] North American Electric Reliability Corporation, "White Paper: Grid Forming Functional Specifications for BPS-Connected Battery Energy Storage Systems," 2023.

[8] U. J. Minnaar, B. Peterson, H. Mostert, J. Rens, and G. Botha, "Power quality grid code compliance for renewable power plants in South Africa," *IET Generation, Transmission & Distribution*, vol. 13, no. 1, pp. 137–144, 2019. [Online]. Available: https://ietresearch.onlinelibrary.wiley.com/doi/abs/10.1049/iet-gtd.2018.5549

[9] B. Nhlapo and K. Awodele, "Review and comparison of the South African grid code requirements for wind generation with the European countries' grid codes," in *2020 International SAUPEC/RobMech/PRASA Conference*, 2020, pp. 1–6.

[10] NERSA, "Grid Connection Code for Battery Energy Storage Facilities (BESF) Connected to the Electricity Transmission System (TS) or the Distribution System (DS) in South Africa," 2021.

[11] G. G. Farivar, W. Manalastas, H. D. Tafti, S. Ceballos, A. Sanchez-Ruiz, E. C. Lovell, G. Konstantinou, C. D. Townsend, M. Srinivasan, and J. Pou, "Grid-connected energy storage systems: State-of-the-art and emerging technologies," *Proceedings of the IEEE*, vol. 111, no. 4, pp. 397–420, 2023.

[12] ESKOM Transmission System Operator, "Certification and performance monitoring for battery energy storage facility reserves," 2023.

[13] R. Li, H. Geng, and G. Yang, "Fault ride-through of renewable energy conversion systems during voltage recovery," *Journal of Modern Power Systems and Clean Energy*, vol. 4, no. 1, pp. 28–39, 2016.